Acta of Bioengineering and Biomechanics
Vol. 24, No. 2, 2022

Original paper
DOI: 10.37190/ABB-02002-2021-02

Encrustation of the ureteral double-J Stents made of styrene/ethylene/butylene and polyurethane before and after implantation

ADAM HALIŃSKI[1], KAMILA PASIK[2], ANDRZEJ HALIŃSKI[3], PAWEŁ HALIŃSKI[3], ALBERTO TRINCHIERI[4], NOOR BUCHHOLZ[4], KATARZYNA ARKUSZ[2]*

[1] Department of Clinical Genetics and Pathology, University of Zielona Góra, Zielona Góra, Poland.
[2] Department of Biomedical Engineering, University of Zielona Góra, Zielona Góra, Poland.
[3] Department of Paediatric Urology, "Klinika Wisniowa", "Cherry Clinic", Zielona Góra, Poland.
[4] Scientific Office, U-merge Ltd., London-Athens-Dubai, Athens, Greece.

Purpose: The aim of this study was to determine the affinity to crystal, calculi and biofilm deposition on ureteral double-J stents (DJ stents) after ureterorenoscopic–lithotripsy procedure (URS-L). The analysis was performed in two aspects: to determine which material used for fabricating ureteral stents promotes encrustation and which part of the DJ stents is the most vulnerable for blockage. *Methods*: One hundred and twenty patients with an indwelling DJ stent duration between 7 and 78 days were included in this study. The encrustation of DJ stents was characterized by scanning electron microscopy (SEM), and the mechanical properties of DJ stents were examined using the standard MTS Micro Bionix tensile test. *Results*: This study showed that polyurethane catheters have a much higher affinity for encrustation than styrene/ethylene/butylene block copolymer. Obtained results indicated the proximal (renal pelvis) and distal (urinary bladder) part is the most susceptible to post-URS-L fragments and urea salt deposition. Both the DJ ureteral stents' outer and inner surfaces were completely covered even after 7 days of implantation. *Conclusions*: Performed analysis pointed out that polyurethane DJ stents have a much higher affinity for encrustation of calculi and NaCl crystals compared to the silicone-based copolymer. The surface of the ureteral stents needs improvement to minimize salt and kidney stone deposition, causing pre-biofilm formation and the occurrence of defects and cracks.

Key words: *Young's modulus, SEM observation, stone disease, urologic surgical procedure, DJ catheter, encrustation*

1. Introduction

A common chronic kidney condition that pertains to urological patients is urolithiasis, leading to urinary stones. The mentioned problem is a common problem with a worldwide estimated 20% prevalence, which is suspected to grow significantly over the coming years [11]. This is estimated to a 5-year recurrence rate of 50%, and the incidence and prevalence of kidney stones are increasing globally [2]. Ureteral obstruction is caused by kidney stones disorder, renal function, and intensifies patient pain [35].

A double-J ureteral stent implantation is a common surgical procedure aiming at ureteral drainage to assure renal function, treat pain caused by ureteral obstruction and avoid external or visible devices [20]. The most common materials used as ureteral stents are polyethylene, polyurethane, and silicone [15], [32]. The type of material affects the patient's body response, hence, the required characteristics such as biocompatible, antimicrobial and antifouling

* Corresponding author: Katarzyna Arkusz, Department of Biomedical Engineering, Institute of Material and Biomedical Engineering, Faculty of Mechanical Engineering, University of Zielona Góra, ul. Licealna 9, 65-417 Zielona Góra, Poland. E-mail: k.arkusz@iimb.uz.zgora.pl
Received: December 21st, 2021
Accepted for publication: May 4th, 2022

[28]. Furthermore, materials required for urinal catheterization are defined by their mechanical properties: low surface roughness [18], high mechanical strength and flexibility [28]. Among these materials, silicone stents may be more advantageous than polyurethane stents due to the lower risk of calcification and prolonged maintenance of tensile strength for up to 20 months [1]. However, no comparable research has been performed yet.

Ureteric stents have been deployed for over four decades, and as their technique is upgrading, their complications have expanded (e.g., stent migration, encrustation, stone formation and fragmentation) [1]. Short-term stenting for stone removal (<6 weeks) represents an immense economic burden. When in contact with urine, ureteral stents frequently become covered by calcium phosphate and calcium oxalate crystal-containing encrustations, which can damage the uroepithelium and pain and have been suspected to promote infections [8], [25]. Hitherto, studies of ureteral stenting included determination of effective urine flow from the kidney to the bladder [13], [14], structural and chemical composition investigation [9], [32], [33], and shape and size optimization [24], [31]. The urine flow consists of in-stent (luminal) and out-of-stent (extraluminal) flows, whereas lower flow rates were observed in larger DJ stents [13] and increasing the number of side holes increased the overall flow rate [14]. Encrustation and pain increase along with the diameter of the indwelling ureter stent [24]. It is important to note that encrustation is a serious complication of ureteral stent use, affecting the removal procedure. The encrustation of ureteral stents may be due to the deposition of organic layers (conditioning film), uropathogens and salts in the urine. Encrustation at the distal end is less than the proximal one and calcium content, which is lower in the distal coil [33]. On the other hand, there can be differences in encrustation composition at each end of a stent [30], [32]. Additionally, the deposition of calculi or crystal promoted biofilm formation, affecting the urinary tract infection [27].

This paper focuses on determining which materials among those commonly used in ureteral stents show the greatest affinity for biofilm formation and which part of the DJ stent is the most vulnerable to kidney stone formation in time. Therefore, there is a need to study the mechanism of formation of kidney stones on the ureteral stent's surface and methods to prevent these processes and study the influence of these structures on the mechanical properties of a ureteral stent.

2. Materials and methods

2.1. Materials

In total, 120 double-J ureteral stents (DJ stents) were removed from renal stone patients and recruited to the study between January 2019 and May 2021. All ureteral stents were obtained from patients who had been diagnosed with calcium oxalate urolithiasis.

First, the most susceptible material for biofilm formation was indicated. DJ stents of two manufacturers were examined 31 days after their initial ureteral placement in adult patients after the ureterorenoscopic – lithotripsy (URS-L) to treat calcium oxalate stone. The first kind of DJ stent was built with a proprietary silicone-modified styrene/ethylene/butylene block copolymer (copolymer DJ stents); the second was a classic polyurethane stent. The polyurethane DJ stent accounted for 25% of all analyzed samples (30 pcs).

Second, the influence of implantation time to encrustation and biofilm formation was examined. The copolymer DJ stents after the URS-L, which implantation period lasted from 7 to 78 days, were examined using scanning electron microscopy. Each of the polyurethane stents were implanted for 31 days (25%, 30 pcs.), while the copolymer DJ stents were implanted for 7 days (8.3%, 10 pcs.), 17 days (11.7%, 14 pcs.), 25 days (8.3%, 10 pcs.), 31 days (35.9%, 43 pcs.) and 78 days (10.8%, 13 pcs.).

2.2. Surface analysis of stents

A microscopic analysis was performed on the ureteral stents implanted after the URS-L. The microscopic observation was performed by the scanning electron field emission microscope JEOL JSM 7600F (SEM). The microscopic analysis of the ureteral stents required an additional sample preparation procedure [3], [25]. The ureteral stent surface was sputtered with a chromium layer with a thickness of 5 nm. Representative polyurethane and copolymer DJ stents before and after implantation for 31 days were characterized by Fourier transform infrared spectroscopy (FTIR) (Thermo Scientific™ Nicolet™ iS50 FTIR Spectrometer, Thermo Scientific™, USA). Data were collected in the absorption mode between 4000 cm^{-1} and 400 cm^{-1} with a resolution of 4 cm^{-1}. Room temperature and humidity during all process were maintained stable at 23 °C and 35%, respectively.

2.3. Mechanical testing of DJ stents

Tensile strength and stiffness were tested for all DJ stents before and after urinary exposure. The tensile strength was measured using an MTS Micro Bionix Testing System with Testworks II software, using a 5 N load cell. DJ stents were tested in uniaxial tension at 1 mm/s for 1 second. A preconditioning run was done for each stent, including a 3-minute hold time at 5 mm with 30 seconds between the preconditioning run and the first trial. Each DJ stent was examined using the tensile test minimum times, keeping the same manner of reposition. Unpaired Student's *t*-test was used for the comparison of the two groups of implantation time for each DJ-stent. A value of $p < 0.05$ was considered statistically significant.

3. Results

3.1. Influence of DJ stent composition on encrustation and fracture

In the beginning, it should be noticed that each of the analyzed DJ stents (120 pct) was divided according to the stent material, implantation time. Each group was managed to the KUB (Kidney, Ureter, Bladder) encrusted ureteral stent scoring system, while the standard deviation in each group did not exceed 1. Then, each DJ stent was divided into three parts (proximal, middle, distal), and the database of SEM pictures of each section was analyzed to choose the most similar and repeated photos, which are presented in this section.

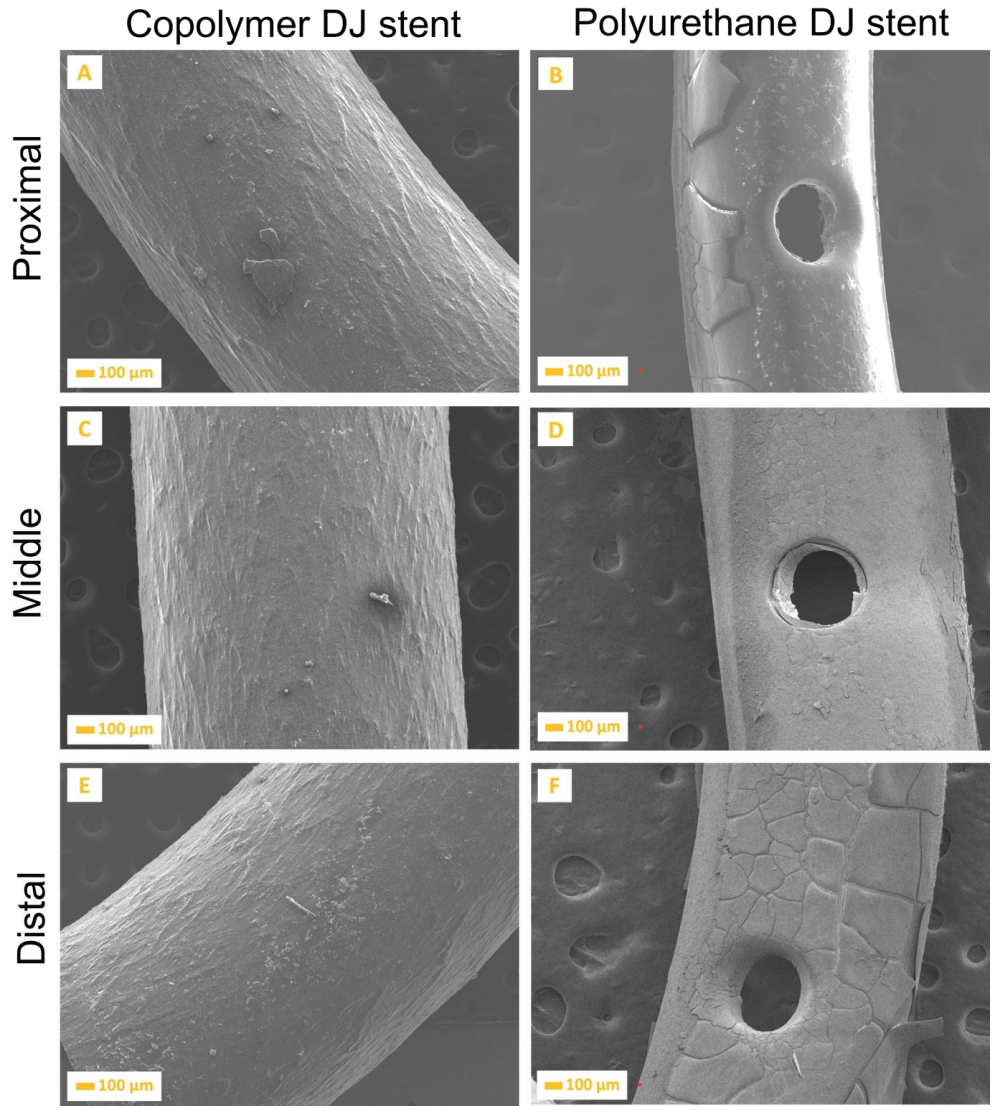

Fig. 1. SEM images of a DJ stent made of styrene/ethylene/butylene block copolymer, and polyurethane, implanted for 31 days

The surface morphologies of DJ stents, made of copolymer and polyurethane, implanted for 31 days in the patient's body, have been investigated using scanning electron microscopy, the results of which are shown in Fig. 1. The proximal part of the DJ stents means "pigtail", placed in the renal pelvis, while the distal coil is placed in the urinary bladder. As shown in Fig. 1, the copolymer DJ stents are covered with a much smaller number of crystals than the polyurethane version. The distal and proximal part of the polyurethane DJ stent is covered with the most complex film presenting a multi-layered structure.

In Figure 2, the data for a representative DJ stent made of styrene/ethylene/butylene block copolymer, and polyurethane, before and after implantation for 31 days by FTIR is presented.

Before the implantation, several IR characteristic peaks were observed for copolymer and polyurethane DJ stents (Figs. 2A, B, respectively). Observed for copolymer DJ stent, the broad peaks around 2949 and 2917 cm^{-1} corresponded to the C–H stretching from the alkyl groups. In the range of 1500–800 cm^{-1}, peaks at 1453 cm^{-1} (C–H bending), 1260 cm^{-1} (C–O stretching), 1100 cm^{-1}–1000 cm^{-1} (C–O stretching in C–O–H groups and COC groups), and 805 cm^{-1} (C–H rocking mode) were observed.

After implantation of copolymer DJ stents for 31 days, new peaks appeared around 3300 cm^{-1} due to the hydrogen-bonded OH stretching vibrations, 1729 cm^{-1} (carbonyl groups), 1697 cm^{-1} (the C=O stretching), and 1597 cm^{-1} (N–H plane stretch), the peak 1104 cm^{-1} (phosphates).

Before the implantation, the IR spectrum for polyurethane DJ stents showed characteristic peaks at 3331 cm^{-1} (stretching of the NH bond), 2948 and 2868 cm^{-1} (alkane –CH stretching vibration), 1727 cm^{-1} – 1700 cm^{-1} (carbonyl absorption band), 1596 cm^{-1} – 1527 cm^{-1} (a shoulder) 1220 cm^{-1} (C–O stretching of the carbonate group), 1174 cm^{-1} (C–N and C–O stretching vibrations), 1111 cm^{-1} and 1065 cm^{-1} (ester C–O–C symmetric stretching vibration).

After implantation for 31 days the new peaks occured at 2919 cm^{-1} (NH_4^+ stretching), 1623 cm^{-1} (the C=O stretching), 1452 cm^{-1} (P=O stretching), 1375 cm^{-1} (C–N stretching), 803 cm^{-1} (C–C stretching), 526 cm^{-1} (O–C–O bending).

The mechanical properties of unused DJ stents and stents retrieved from patients following insertion from 7 to 31 days are presented in Fig. 3. The Young's modulus (E) was calculated for each DJ stent using engineering stress, which assumes no cross-sectional area changes. The DJ stent's mechanical strength made of polyurethane (E = 628 ± 21 kPa) was twice lower compared to copolymer one (E = 1547 ± 129 kPa). After implantation, the copolymer DJ stent was the stiffest and the DJ stent implanted for 31 days was characterized by the lowest stiffness (E = 1065 ± 90 kPa). Implantation caused the significant loss of mechanical strength of polyurethane DJ stents to a value of 325 ± 10 kPa. There was no significant change in

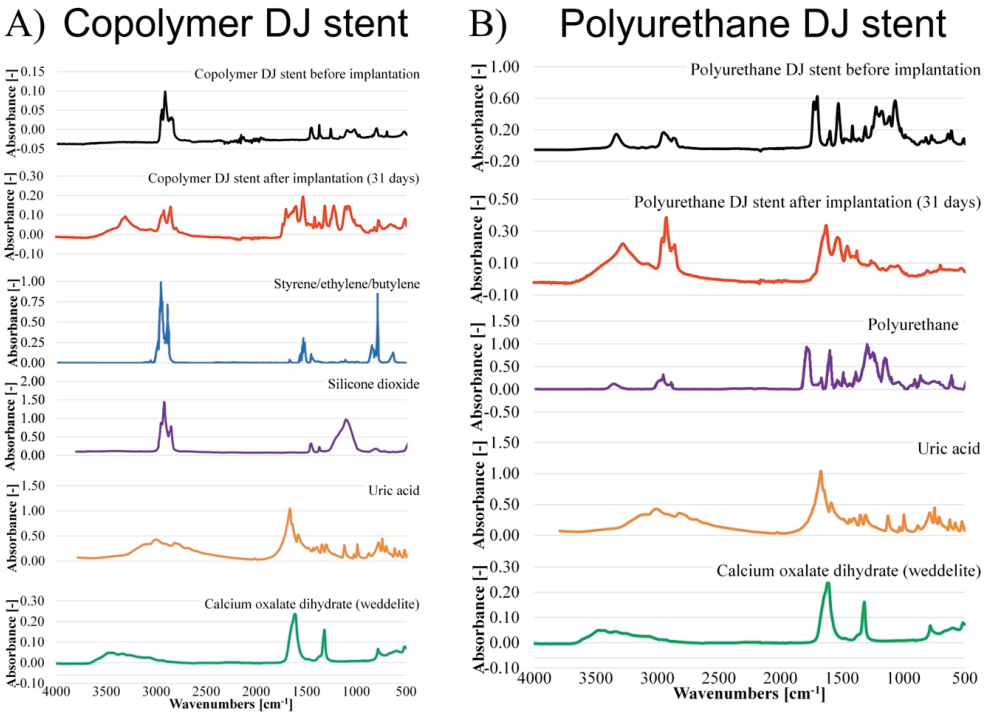

Fig. 2. FTIR spectra of a DJ stent made of styrene/ethylene/butylene block copolymer, and polyurethane, implanted for 31 days

the ultimate force of ureteral stents following implantation during 25 days in comparison to 31 days for copolymer DJ stents.

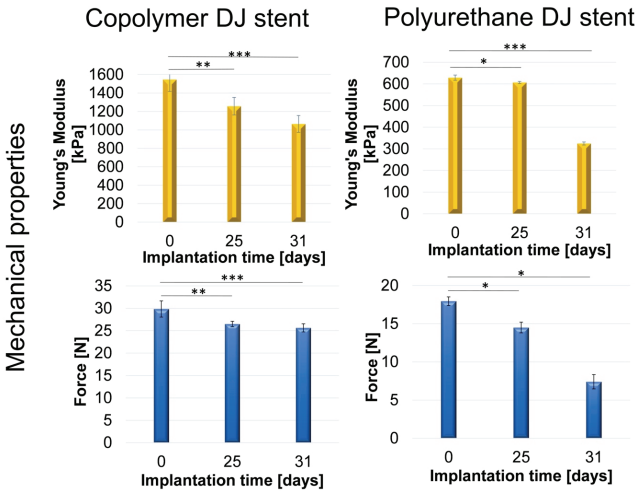

Fig. 3. SEM images of a DJ stent made of styrene/ethylene/butylene block copolymer, and polyurethane, implanted for 31 days,
* $p < 0.05$, ** $p < 0.005$, *** $p < 0.001$

3.2. Mechanism of stone formation on DJ stent surface

The outer and inner side of the copolymer DJ stents proximal parts, which were removed from the patients' bodies after 7, 17, and 78 days are shown in Fig. 4. The outer side of the proximal part of the DJ stents is covered over time – the thickness of this layer increased with the implantation period's increase. The most extensive agglomeration on the inner side was observed during the seventh day of implantation (Fig. 4B). The extension of implantation time leads to a continuous increase of the multilayer's thickness on the inner side of the proximal part of the DJ stents (Fig. 4D) until 17 days of implantation, and thereafter its further acceleration (Fig. 4F).

The encrustation of the distal part of the DJ stents in varying time of implantation was shown in Fig. 5. During the first day of implantation, the outer (Fig. 5A) and inner (Fig. 5B) side of DJ stents were completely covered by the multilayer of calcium oxalate fragments.

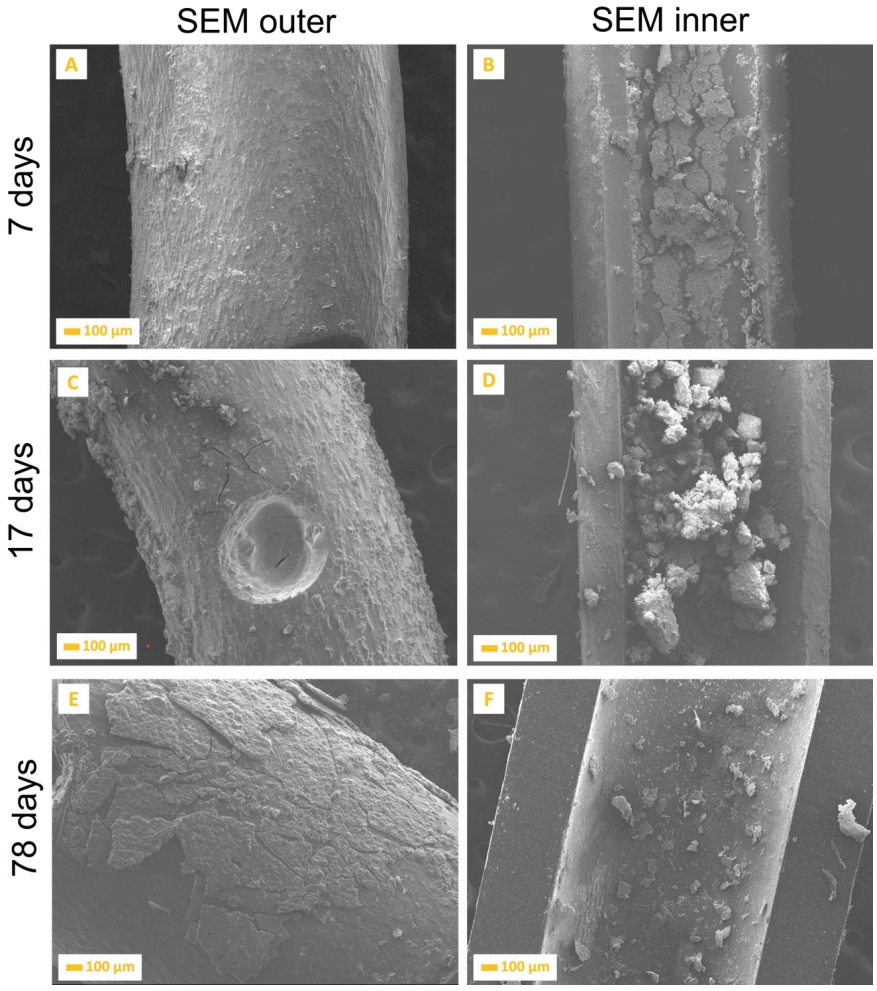

Fig. 4. SEM images of a proximal part of DJ stents implanted for 7–78 days

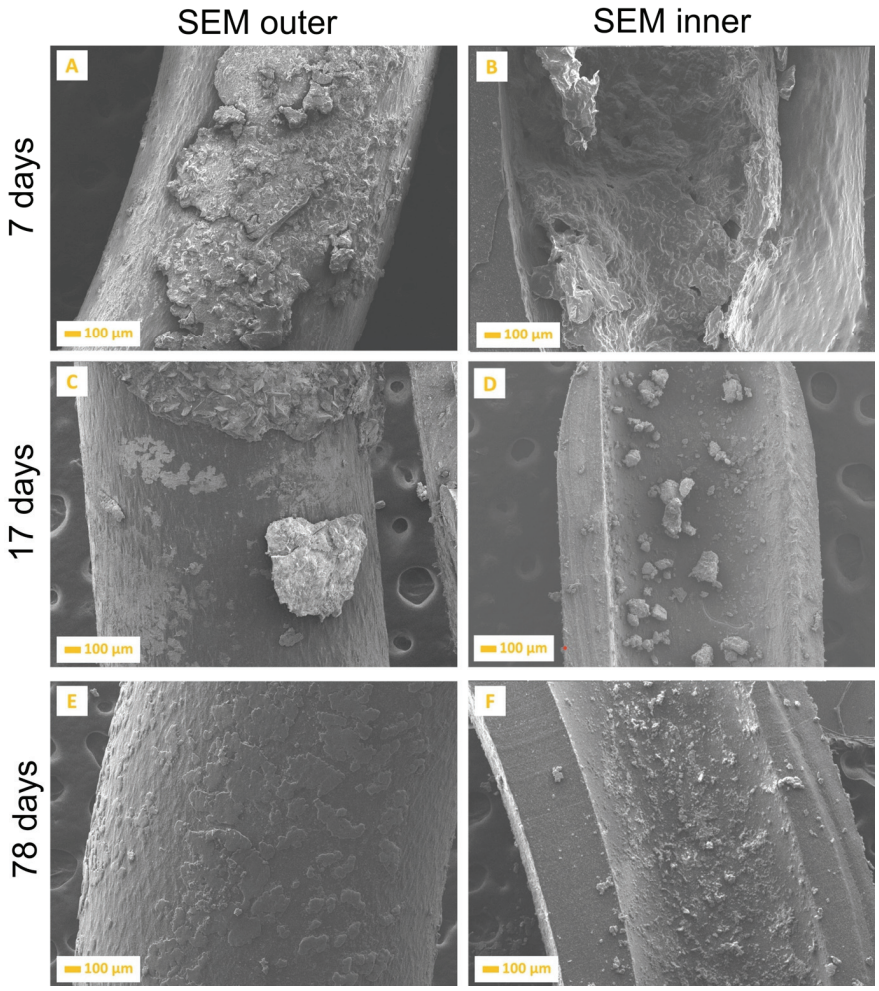

Fig. 5. SEM images of a distal part of DJ stents implanted for 7–78 days

Extension of implantation time resulted in forming a compact layer, leading to pain and difficult removal. After 78-days implantation, the outer (Fig. 5E) and inner (Fig. 5F) side was completely covered by small calculus growing on one another.

4. Discussion

Prevention of stone-crystal-layer formation on DJ stents is essential due to increased pressure in the blocked stent, causing many clinical problems, such as vesicoureteral reflux, migration, encrustation, urinary infection, stent fracture, necrosis and ureteroarterial fistula [28], [35].

The first stage of research was to determine the influence of DJ stents composition on encrustation. As shown in Fig. 1, the distal and proximal part of the polyurethane DJ stent is covered with the most complex film presenting a multi-layered structure. This encrustation was classified as score 4 for polyurethane stents and as score 2 for copolymer stents on a scale for scoring encrustations on ureteral double-J stents elaborated by Roupret [30].

Further, the FTIR analysis (Fig. 2) was performed to characterize encrustations, especially identifying the calculi adsorbed components onto the DJ stent's surface. According to the literature, about 30 distinct components have been found in urinary calculi [36]. Thus, we decided to compare the obtained IR spectrum only for the main component of urea and urinary calculi.

For copolymer DJ stent before implantation, as it can be seen in Fig. 2A, the main absorption peak in IR spectrum appeared in the wavenumber: 2429 cm^{-1}, 1453 cm^{-1}, 805 cm^{-1} confirmed the styrene/ethylene/butylene structure, and the silicone covering by the presence of a peak in 2917 cm^{-1}, and 1100 cm^{-1} – 1000 cm^{-1}. The FTIR spectra of the polyurethane DJ stents (Fig. 2B) confirmed the polyurethane structure with the typical carbonyl absorption band of the ester bond located at 1729 cm^{-1}, and a shoulder at 1697 cm^{-1}, which can be attributed to the urethane and urea carbonyl groups.

The absorbance at 3300 cm^{-1} is consistent with the stretching of the NH bond and is characteristic for the urethane and urea groups. The other characteristic bands are 2900 cm^{-1} due to the alkane –CH stretching vibration, 1174 cm^{-1} due to the coupled C–N and C–O stretching vibrations, and 1062 cm^{-1} due to the ester C–O–C symmetric stretching vibration.

As shown in Figs. 2A and B, the peak intensity of the IR spectra changed significantly after the implantation of copolymer and polyurethane DJ stents. After the implantation of copolymer DJ stent for 31 days, the absorbed encrustation was identified mainly as calcium oxalate dihydrate (weddellite), characterized by four sharp peaks between wavenumbers 1600 cm^{-1} – 777 cm^{-1}. Furthermore, the peak of 2918 cm^{-1} (N–H stretching) indicated the presence of NH4+ (ammonium ion); therefore, the stone may be included in the type of ammonium ion calcium oxalate dihydrate, or the uric acid crystal may be absorbed onto the DJ surface. A peak that characterizes calcium oxalate kidney stone type was also found in the encrusted layer after 31 days of polyurethane DJ stents implantation.

Secondly, the influence of implantation time on mechanical degradation was briefly described in the literature comparing the tensile strength of varying types of DJ stents [12], [29]. To the best of our knowledge, only Gorman et al. [10] performed an analysis of the influence of implantation time on the mechanical strength of DJ stents. However, this research was carried out on polyethylene stents and in artificial fluid. In this paper, the preconditioning procedure relied on the results presented in the literature [21]. Subjecting the samples to cyclic loads that do not break them stabilizes their reactions before tested tension. Preconditioning helps to eliminate variable sample responses to a given load and achieve a steady state. The procedures applied to provide a reproducible mechanical response that is the basis of reliable results for analysis. Obtained results showed that increased implantation time caused a decrease in Young's modulus (Fig. 3), indicating that decreased stent rigidity had occurred. Loss of mechanical properties of polyurethane DJ stents results in lower ultimate force at its break. These observations clearly indicate higher stability and less degradation of copolymer DJ stents implanted for 31 days. It also excludes the possibility of long-term use of polyurethane DJ stents. Moreover, the build-up of deposits on the stent surface causes increasing stiffness and greater susceptibility to cracks and fractures. These results are in accordance with several studies [7], [12], [25], [29]. Highly elastic and flexible materials are more likely to crack or bend *in vivo*, while more rigid materials could cause severe bladder urgency, hematuria, or fracture during long-term stenting [23], [34].

Additionally, the proximal and distal parts (Fig. 1) are more likely to be exposed to contact with the urea, which results in its element deposition. According to the lower encrustation of copolymer DJ stents, these stents were chosen to further research. The previous investigation on flow and encrustation of DJ stents pointed out that long-term stent use is associated with precipitation of salts from the urine and infection, leading to a build-up of crystalline deposits on the stent surface, resulting difficult and painful stent removing [8], [20], [28], [30], [32].

The obtained results showed that the DJ stents' inner and outer surfaces were covered and deposited with the crystals of urea and, more importantly, by the post-URS-L fragments. The outer and inner side of the proximal (Fig. 4) and distal (Fig. 5) parts of the copolymer DJ stents, which were removed from the patients' bodies after 7, 17, and 78 days were covered with a more complex, multilayer consisting mostly of precipitated crystals (NaCl) and post-URS-L fragments (calcium oxalate stone). Performed analysis showed that the encrustation at the distal end (Fig. 5) was less than the proximal one (Fig. 4) and calcium content, which was lower in the distal coil. This hypothesis is confirmed by the work of Sighinolf et al. [33] and Kim et al. [14], who suggest that the last side hole in the proximal coil of the stent, located in the renal pelvis and the first side hole of the shaft of the stent, located in the even side hole throughout the ureter is critical to a DJ stent to maximize its role in the upper urinary system. Similar observations were made with hemodialysis catheters in our previous research [15], [25]. The encrustation on the distal and proximal parts of copolymer DJ stents formed during the first 17 days after implantation was classified as score 6 on a scale for scoring encrustations [30]. Such a distribution of film components suggests that the ureteral stent's blockage is due to not only large kidney stones but also a continuous flow of small calculi growing on one another. The most extensive agglomeration was observed during the seventh day of implantation (Fig. 4B), which could be the result of cleaning the kidney of post-URS-L residues. This is a crucial moment in the blockage of the DJ stents. If the DJ stent diameter is too large, the flow rates are too low, extending the contact time of post-URS-L fragments with the surface of DJ stents, resulting in its blockage. If the diameter of the DJ stent has been chosen correctly, the extension of implantation time results in a continuous increase of the thickness of the multilayer on the inner side of the proximal part of the

DJ stents (Figs. 3D and 3F). Additionally, the calculi or crystal deposition promotes biofilm formation, which affects the urinary tract infection [13]. Performed results and previous research [6], [22] indicate the necessity to use antibacterial and anticoagulation coatings of DJ stents, such as nano-silver [4], metallic nanoparticles [26], nitrofurazone [19], chlorhexidine [37], polytetrafluoroethylene (PTFE), hydrogel [17], lysostaphin [16] and antibacterial and anticoagulation coatings [5].

5. Conclusions

Previous studies of DJ stents were performed to the material selection for biocompatibility and optimization of their shape to ensure free urine flow. The literature indicates the importance of side holes in the DJ stents and their impact on stents clogging, however, ignoring the impact of the material itself and implantation time.

This study showed that polyurethane DJ stents have a much higher affinity for encrustation of calculi compared to the silicone-based copolymer. Residues deposited on the surface form a homogeneous multilayer, mainly composing of weddellite and uric acid crystal, which close the DJ stents' lumen and significantly affect the flow of urine. Further analysis showed that the most vulnerable segment is the proximal part of the DJ stent (the part located in the renal pelvis). Slightly fewer fragments of kidney stones and sodium crystals are deposited in distal section of the stents. Studies have shown that as soon as seven days after implantation, the DJ stents may be completely blocked if its diameter is not properly adjusted. It has been observed that the layer formed on the outer surface of the catheter increases with longer implantation time, which occurs faster than for the inner layer. Implantation results in loss of mechanical strength of polyurethane DJ stents after just 31 days, what explains the problem of cracking/damage of DJ stents in patients' body or in removing procedure.

The surface of the ureteral stents needs improvement to minimize salt and kidney stone deposition, causing pre-biofilm formation and the occurrence of defects and cracks.

References

[1] AHALLAL Y., KHALLOUK A., JAMAL EL FASSI M., FARIH M.H., *Risk Factor Analysis and Management of Ureteral Double-J Stent Complications*, Rev. Urol., 2011, 12 (2–3), 147–151.

[2] AKRAM M., IDREES M., *Progress and prospects in the management of kidney stones and developments in phyto-therapeutic modalities*, Int. J. Immunopathol. Pharmacol., 2019, 33, 1–5.

[3] ARKUSZ K., KRASICKA-CYDZIK E., *The effect of phosphates and fluorides, included in TiO_2 nanotubes layers on the performance of hydrogen*, Arch. Metall. Mater., 2018, 63 (2), 1–8.

[4] ARKUSZ K., NYCZ M., PARADOWSKA E., PIJANOWSKA D.G., *Electrochemical stability of TiO_2 nanotubes deposited with silver and gold nanoparticles in aqueous environment*, Environ. Nanotechnol. Monit. Manag., 2021, 15, 1–12.

[5] ARKUSZ K., PARADOWSKA E., NYCZ M., MAZUREK-POPCZYK J., BALDY-CHUDZIK K., *Evaluation of the Antibacterial Activity of Ag- and Au-Nanoparticles Loaded TiO_2 Nanotubes*, J. Biomed. Nanotech., 2020, 16 (9), 1416–1425.

[6] ARKUSZ K., PASIK K., HALIŃSKI A., HALIŃSKI A., *Surface analysis of ureteral stent before and after implantation in the bodies of child patients*, Urolithiasis, 2020, 1–10.

[7] BARTKOWIAK-JOWSA M., BĘDZIŃSKI R., SZARANIEC B., CHŁOPEK J., *Mechanical, biological and microstructural properties of biodegradable models of polymeric stents made of PLLA and alginate fibers*, Acta Bioeng. Biomech., 2011, 13 (4), 21–8.

[8] BUHMANN M.T., ABT D., NOLTE O., *Encrustations on ureteral stents from patients without urinary tract infection reveal distinct urotypes and a low bacterial load*, Microbiome, 2019, 7 (60), 1–17.

[9] DAVENPORT K., KUMAR V., COLLINS J., MELOTTI R., TIMONEY A.G., KEELEY F.X., *New Ureteral Stent Design Does Not Improve Patient Quality of Life: A Randomized, Controlled Trial*, J. Urol., 2011, 185 (1), 175–178.

[10] GORMAN S.P., JONES D.S., BONNER M.C., AKAY M., KEANE P.F., *Mechanical performance of polyurethane ureteral stents in vitro and ex vivo*, Biomaterials, 1997, 18 (20), 1379–1383.

[11] HALIŃSKI A., HALIŃSKI A.H., *Stone located in proximal part of the ureter – ESWL, URS-L, flexible URS, MicroPerc? Which approach should we choose in children-prospective study*, Eur. Urol. Suppl., 2017, 16 (7), 2549.

[12] HENDLIN K., DOCKENDORF K., HORN C., PSHON N., LUND B., MONGA M., *Ureteral stents: Coil strength and durometer*, Urology, 2006, 68 (1), 42–45.

[13] KIM K., KIM H., CHOI Y.H., LEE S.B., BABA Y., *Urine flow analysis using double J stents of various sizes in in vitro ureter models*, Int. J. Numer. Method., 2020, 36 (6), 1–12.

[14] KIM K.W., KIM H.H., CHOI Y.H., LEE S.B., BABA Y., SUH S.H., *Arrangement of side holes in a double J stent for high urine flow in a stented ureter*, J. Mech. Sci., 2020, 34 (2), 949–954.

[15] KLOSKOWSKI T., JUNDZIŁ A., KOWALCZYK T., U*reter Regeneration–The Proper Scaffold Has to Be Defined*, PLoS One, 2014, 9 (8), 1–13.

[16] KOTASKOVA I., OBRUCOVA H., MALISOVA B., VIDENSKA P., ZWINSOVA B., PEROUTKOVA T., FREIBERGER T., *Molecular techniques complement culture-based assessment of bacteria composition in mixed biofilms of urinary tract catheter-related samples*, Front. Microbiol., 2019, 10, 462.

[17] KUROWIAK J., KACZMAREK-PAWELSKA A., MACKIEWICZ A.G., BĘDZIŃSKI R., *Analysis of the Degradation Process of Alginate-Based Hydrogels in Artificial Urine for Use as a Bioresorbable Material in the Treatment of Urethral Injuries*, Processes, 2020, 8 (3), 304.

[18] LAWRENCE E.L., TURNER I.G., *Materials for urinary catheters: a review of their history and development in the UK*, Med. Eng. Phys., 2005, 27 (6), 443–453.

[19] LO J., LANGE D., CHEW B., *Ureteral stents and foley catheters-associated urinary tract infections: the role of coatings and materials in infection prevention*, Antibiotics, 2014, 3 (1), 87–97.

[20] MILICEVIC S., BIJELIC R., JAKOVLJEVIC B., *Encrustation of the Ureteral Double J Stent in Patients with a Solitary Functional Kidney – a Case Report*, Med. Arh., 2015, 69 (4), 265–268.

[21] MILLER K.S., EDELSTEIN L., CONNIZZO B.K., SOSLOWSKY L.J., *Effect of Preconditioning and Stress Relaxation on Local Collagen Fiber Re-Alignment: Inhomogeneous Properties of Rat Supraspinatus Tendon*, J. Biomech. Eng., 2012, 134 (3), 031007.

[22] MOSAYYEBI A., MANES C., CARUGO D., *Advances in Ureteral Stent Design and Materials*, Curr. Urol. Rep., 2018, 19 (35), 1–9.

[23] MOSAYYEBI A., VIJAYAKUMAR A., YUE Q.Y., BRES--NIEWADA E., MANES C., CARUGO D., SOMANI B.K., *Engineering solutions to ureteral stents: material, coating and design*, Cent. European J. Urol., 2017, 70, 270–274.

[24] NESTLER S., WITTE B., SCHILCHEGGER L., JONES J., *Size does matter: ureteral stents with a smaller diameter show advantages regarding urinary symptoms, pain levels and general health*, World J. Urol., 2019, 38 (4), 1059–106.

[25] NYCZ M., PARADOWSKA E., ARKUSZ K., KUDLIŃSKI B., KRASICKA-CYDZIK E., *Surface analysis of long-term hemodialysis catheters made of carbothane (poly(carbonate)urethane) before and after implantation in the patients' bodies*, Acta Bioeng. Biomech., 2018, 20 (2), 47–53.

[26] NYCZ M., PARADOWSKA E., ARKUSZ K., PIJANOWSKA D.G., *Influence of geometry and annealing temperature in argon atmosphere of TiO_2 nanotubes on their electrochemical properties*, Acta Bioeng. Biomech., 2020, 22 (1), 165–177.

[27] OZGUR B.C., EKICI M., YUCETURK C.N., BAYRAK O., *Bacterial colonization of double J stents and bacteriuria frequency*, Kaohsiung J. Med. Sci., 2013, 29 (12), 658–661.

[28] PAWLIKOWSKI M., SKALSKI K., SOWIŃSKI T., *Hyper-elastic modelling of intervertebral disc polyurethane implant*, Acta Bioeng. Biomech., 2013, 15 (2), 1–8.

[29] PEDRO R.N., HENDLIN K., KRIEDBERG C., MONGA M., *Wire-Based Ureteral Stents: Impact on Tensile Strength and Compression*, Urology, 2007, 70 (6), 1057–1059.

[30] ROUPRÊT M., DAUDON M., HUPERTAN V., GATTEGNO B., THIBAULT P., TRAXER O., *Can ureteral stent encrustation analysis predict urinary stone composition?*, Urology, 2005, 66 (2), 246–251.

[31] SALI G.M., JOSHI H.B., *Ureteric stents: Overview of current clinical applications and economic implications*, Int. J. Urol., 2019, 27 (1), 7–15.

[32] SCARNECIU I., BRATU O.G., COBELSCHI C.P., *The Risk Factors and Chemical Composition of Encrustation of Ureteral Double J Stents in Patients with Urolithiasis*, Rev. Chim., 2018, 69 (12), 3406–3409.

[33] SIGHINOLFI M.C., SIGHINOLFI G.P., GALLI E., MICALI S., FERRARI N., MOFFERDIN A., BIANCHI G., *Chemical and Mineralogical Analysis of Ureteral Stent Encrustation and Associated Risk Factors*, Urology, 2015, 86 (4), 703–706.

[34] SINGHA P., LOCKLI J., HANDA H., *A review of the recent advances in antimicrobial coatings for urinary catheters*, Acta Biomater., 2017, 50, 20–40.

[35] WANG Y., ZHONG B., YANG X., WANG G., HOU P., MENG J., *Comparison of the efficacy and safety of URSL, RPLU, and MPCNL for treatment of large upper impacted ureteral stones: a randomized controlled trial*, BMC Urol., 2017, 17 (1), 1–7.

[36] WARTY Y., HARYANTO F., FITRI L., HAEKAL M., HERMAN H., *A Spatial Distribution Analysis on the Deposition Mechanism Complexity of the Organic Material of Kidney Stone*, J. Biomed. Phys. Eng., 2020, 10 (3), 273–282.

[37] ZELICHENKO G., STEINBERG D., LORBER G., FRIEDMAN M., ZAKS B., LAVY E., DUVDEVANI M., *Prevention of initial bioflm formation on ureteral stents using a sustained releasing varnish containing chlorhexidine. Vitro study*, J. Endourol., 2013, 27 (3), 333–337.